Monograph:

Zalzala, A.M.S. and Wang, Q. (1997) Comparisons of Case Studies for Optimised Robot Motion. Research Report. ACSE Research Report 668 . Department of Automatic Control and Systems Engineering

Department of
AUTOMATIC
CONTROL
and SYSTEMS
ENGINEERING
UNIVERSITY of SHEFFIELD

COMPARISONS OF CASE STUDIES FOR OPTIMISED ROBOT MOTION

A.M.S. Zalzala and Q. Wang

Robotics Research Group
Department of Automatic Control and Systems Engineering
The University of Sheffield
Mappin Street, Sheffield S1 3JD, United Kingdom

Research Report #668
13 February 1997

Tel : +44 (0)114 2225250
Fax : +44 (0)114 2731729
EMail : rrg@sheffield.ac.uk
Robotics Research Group

Comparisons of Case Studies for Optimised Robot Motion

A. M. S. Zalzala and Q. Wang
Robotics Research Group
Department of Automatic Control and Systems Engineering,
The University of Sheffield,
P.O. Box 600, Mappin Street, Sheffield S1 3JD, United Kingdom
Tel: ++44 (0)114 2225250; Fax: ++44 (0)114 2731729; Email: rrg@sheffield.ac.uk

Abstract: The purpose of this report is two fold. In addition to addressing the formulation of a dynamic scaling approach for use in a genetic-based robot motion planner, the report presents comprehensive comparisons between genetic motion planners and other heuristic/dynamic control methods. The simulations show favourable efficiency and motion optimality in applying the genetic approach for both two and six degree-of-robot arms.

1. INTRODUCTION

A well established approach for robot motion planning employs an exhaustive heuristic technique to search the work space of the arm. The main idea of the algorithm is to tessellate joint space into a grid of possible motion nodes where at each option node, given the position and velocity at the previous node, possible velocity values are constrained by the dynamics of the arm. The most comprehensive formulation is reported by Sahar and Hollerbach (1986), where the full dynamic model of a manipulator and actuator torque limits were both taken into consideration in arriving at the time-optimal trajectory. However, the complexity of this approach is $O(4^n)$, n being the grid size, which results in very heavy computational burden for on-line operation. This estimation is given for 2-joint arms only with a simple tessellation (only three directions are allowed to move from each node). Therefore, the complexity of the approach increases exponentially with the number of joints. Another shortfall of the method is that it neglects the important effects of path curvature (Shiller and Dubowsky (1989)). Here the authors solved the problem by a new scheme to generate the paths. Like Sahar and Hollerbach (1986), tessellation of the joint space is used. However, there is no intention to snap to the grid. Smooth path is generated with brief reference to the tessellation grid with respecting to zero initial and final velocity requirements.

The Robotics Research Group at the University of Sheffield has been involved in extensive investigations of the potential use of genetic algorithms in the motion planning of robotic systems (both off-line and on-line) [1-9]. In an initial assessment [1,2] it was reported that for a grid size of 10x10, the search time for the exhaustive method took more than twenty hours on a Unix based workstation while GAs only took about one hour. Past work by the authors has led to the formulation of an efficient genetic optimisation method implemented for the PUMA 560 arm. The formulations are reported earlier [7-9] including an actual implementation in real-time [6].

In this report, simulation results of the genetic-based motion are compared to results given by earlier published work by other researchers. In addition to [...] above, the work of Dissanayake et al (1991) is considered where a theoretical control approach with some computational techniques is used. Like many conventional numerical methods, the technique proposed takes up an excessive amount of computing time. Much better results with much less computational cost can be achieved using the genetic-based search method with a simple heuristic technique, as reported here.

2. THE MATHEMATICS MODEL OF THE ARM

In Fig. 1, l_{c1} and l_{c2} are the mass centre distances, I_1 and I_2 are the inertia of link 1 and link 2 around their mass centres respectively and m_3 is the payload which is zero in this simulation. The Lagrange-Euler equations can be expressed by a simplified formula as follows:

$$\tau_1 = (d_1 + d_2\cos(\theta_2))\ddot{\theta}_1 + (d_3 + d_4\cos(\theta_2))\ddot{\theta}_2 - d_4\sin(\theta_2)\dot{\theta}_2^2 - 2d_4\sin(\theta_2)\dot{\theta}_1\dot{\theta}_2 + d_5\cos(\theta_1) + d_6\cos(\theta_1 + \theta_2) \qquad (1)$$

$$\tau_2 = (d_3 + d_4\cos(\theta_2))\ddot{\theta}_1 + d_3\ddot{\theta}_2 + d_4\sin(\theta_2)\dot{\theta}_1^2 + d_6\cos(\theta_1 + \theta_2)$$

In equation (1), τ_1 and τ_2 are joint torques, θ_1 and θ_2 are joint angles (please note that q is also used as joint angles in this paper). Where d_1 to d_6 are constant parameters. Both Coulomb and viscous friction are not taken into account for each joint. Table 1 shows two set values for the parameters in equation (1), as reported by Sahar and Hollerbach (1986) and Dissanayake et al (1991).

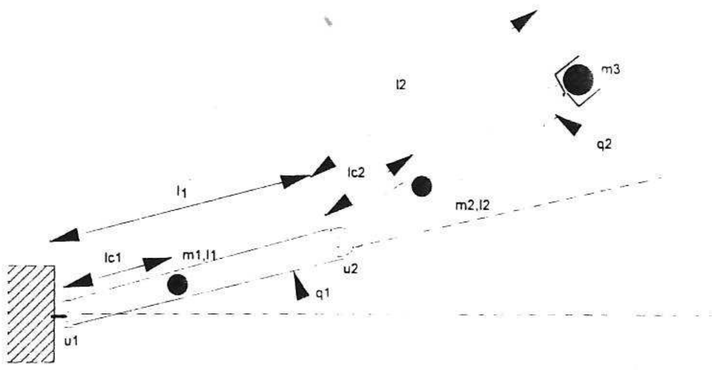

Fig.1. The 2 DOF manipulator used for simulations

Table 1. Parameters of two arm models

	d_1	d_2	d_3	d_4	d_5	d_6
Sahar et al (1986)	20.5	7.5	4.875	3.75	269.5	73.5
Dissanayake (1991)	0.32	0.08	0.12	0.04	0.0	0.0

3. THE DYNAMIC SCALING SCHEME

First formulated in Hollerbach (1984), this is a scheme which makes most out of the joint actuator's capability. When torque values are smaller than their assigned bounds, motion should be speeded up, whereas when any one of the torque values exceeds its bound, motion should be slowed down to avoid violating the actuator's limitations. Thus, by intuition, one can deduce that at least one of the joints is at its bound all the time to obtain the quickest motion. A corner smoothing heuristic technique to help the time-optimal search was presented in Sahar and Hollerbach (1986) by which the direction, but not the magnitude of the velocity vector at the corner point was re-defined. This technique contributed to some extent to forcing a nearly straight-line solution in joint space, which is particularly true if an additional penalty were placed on the redefinition of the velocity at a corner point.

A heuristic is introduced in this report in order to speed up the search. The technique is based on the assumption that, during the whole motion, the joint torque only switch once. This is true for free motion where the shape of the Cartesian space trajectory is of no particular concern. A population of trajectories is generated by the formulated genetic method, forming the trajectory chromosomes. From these trajectories, it is possible to calculate the travel time required for each of them by the dynamic scaling scheme, as summarised by the following steps.

1. For a particular trajectory, the average velocity and acceleration of the jth segment are calculated as

$$\dot{\theta}_j = \frac{\Delta\theta_j}{h_j} \qquad (2)$$

$$\ddot{\theta}_j = \frac{2}{h_j}\left(\frac{\Delta\theta_j}{h_j} - v_{j-1}\right) \qquad (3)$$

where $\Delta\theta_j$ is the joint angular displacement of *j*th segment, h_j is the time interval chosen before the dynamic scaling (equals 1 for sake of simplicity), while v_{j-1} is the final velocity of the previous segment (not the average speed). These calculations are carried out for all joints.

2. The joint torques τ can then be calculated using the dynamics equation (1) for the two DOF arm (or higher such as the PUMA). The dynamic scaling scheme is then used to find the more suitable time interval:

$$(\bar{h}_j)^2(\tau_b - g) + \bar{h}_j(2H.v_{j-1}) - [(h_j)^2(\tau - g) + 2h_j H.v_{j-1}] = 0 \qquad (4)$$

where τ_b is the vector of given torque bounds and g is the gravitational torque but not the gravity constant (refer to Sahar and Hollerbach (1986)).

3. Solve for each of the bounds (for all joints) to find all possible new time intervals Caution is in order in the solving of quadratic equation (4) where if both solutions are valid (i.e. larger than zeros), the smaller value should be chosen. The bound is deemed not possible if both solutions are invalid.

4. The new torque $\bar{\tau}$ for the new time interval can be found out by scaling the old torque τ as follows:

$$\bar{\tau} = \left(\frac{h_j}{\bar{h}_j}\right)^2 (\tau - g) + g + 2\frac{h_j - \bar{h}_j}{(\bar{h}_j)^2} H.v_{j-1} \qquad (5)$$

5. From the time/torque combinations that do not exceed the bounds, choose the shortest time interval for *j*th segment if *j* is smaller than the switch position for acceleration. If *j* is larger, the largest time interval should be chosen among the possible time intervals to indicate deceleration. This heuristic approach, in the authors' experience, is necessary in helping to bring down the end-velocity to near zero and increase the search speed, as there is no time spent in a sorting loop.

6. Recalculate the average velocities and accelerations from equations (2,3) using the new time interval.

7. The new permitted velocities at the end of the current segment can be calculated based on the previous value of the former segment v_{j-1}, current segment acceleration $\ddot{\theta}_j$ and the new time interval $\bar{h}_j$

$$v_j = \ddot{\theta}_j \bar{h}_j + v_{j-1} = \frac{2\Delta\theta_j}{\bar{h}_j} - v_{j-1} \qquad (6)$$

8. Repeat the above steps until *j=n-1*.

For the last segment, special attention should be paid in order to bring down the end velocity to zero. From equation (6), the last time interval should be

$$\bar{h}_n = \frac{2\Delta\theta_n}{v_{n-1}}$$

to ensure v_n to be zero. If $\bar{h}_n$ is larger than zero, and the resulting torques are within their bounds, no dynamic scaling is necessary for the last segment.

4. SIMULATION RESULTS

Detailed simulation results are presented for Dissanayake et al (1991) case 1, Sahar and Hollerbach (1986) case 1 and a real industrial robot arm, the PUMA560. Since the available literature reports results for the 2-joint robot only, no comparisons are included for the PUMA.

4.1 Detailed results for Dissanayake — case 1

In this simulation case, gravitation is not taken into consideration. The joint actuators' bound torques are: $(\pm10;\pm10)$. The maximum generation size was chosen as 600. The best objective found was 0.4046 seconds at iteration 462. The best switch position was found to be near the middle of the time axis of the grid. Total search time was around ten minutes on the Unix workstation.

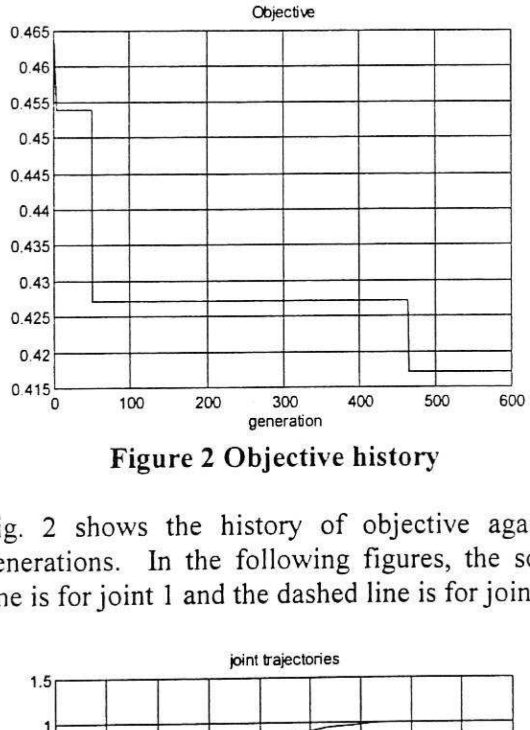

Figure 2 Objective history

Fig. 2 shows the history of objective against generations. In the following figures, the solid line is for joint 1 and the dashed line is for joint 2.

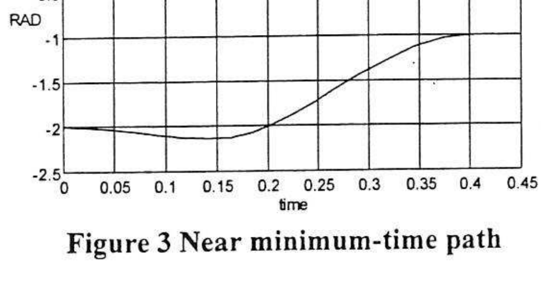

Figure 3 Near minimum-time path

Fig. 3 shows the near time-optimal trajectories searched by GAs, where joint 2 moves inwards resulting in reduced inertia and allowing joint 1 to move faster.

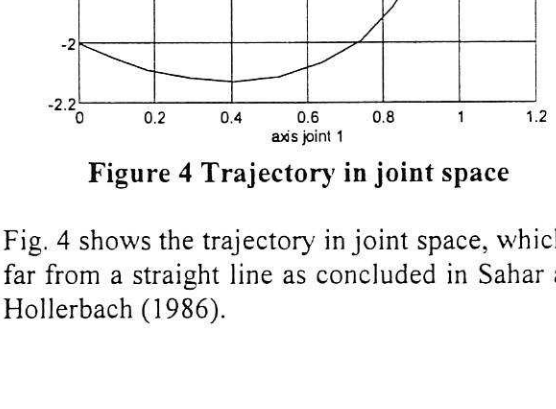

Figure 4 Trajectory in joint space

Fig. 4 shows the trajectory in joint space, which is far from a straight line as concluded in Sahar and Hollerbach (1986).

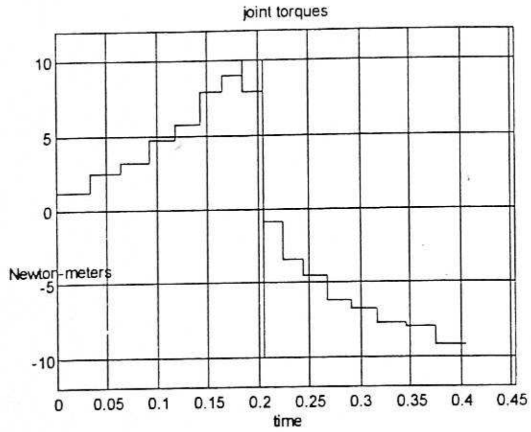

Figure 5 Joint torque information

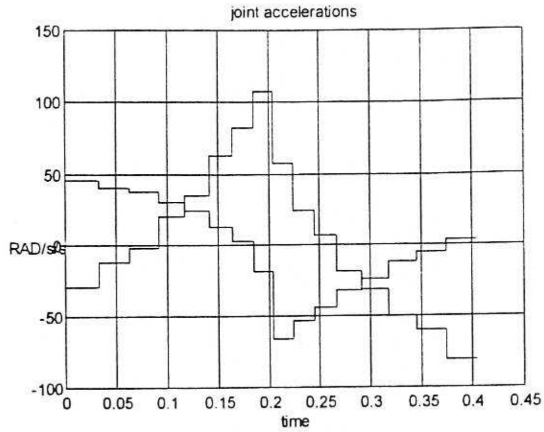

Figure 6 Joint accelerations

Fig. 5 shows the torque information, with all values less than or equal to their limit boundaries. Joint 1 only enjoy the bang-bang motion and is always at its extreme value (except for the last segment), confirming the GAs to have successfully found the global minimum.

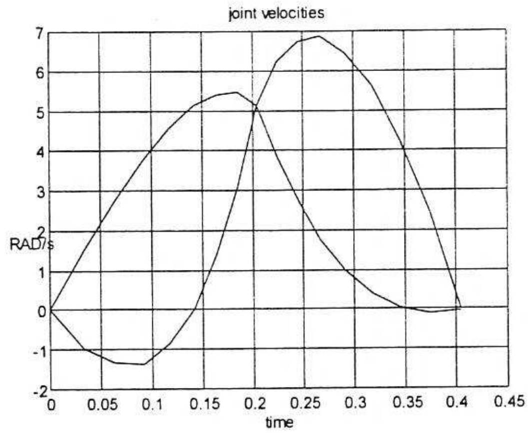

Figure 7 Joint velocities

Fig. 8 shows the joint accelerations, while Fig. 9 shows the joint velocities. Note that the end speed are all almost zeros.

	Initial	positions	Final	positions		
	θ_{10} (RAD)	θ_{20} (RAD)	θ_{1f} (RAD)	θ_{2f} (RAD)	Reported results	Authors' results
Case 1	0.00	-2.00	1.00	-1.00	0.6711	0.4046
Case 2	1.00	-1.00	0.00	-2.00	0.6732	0.4123
Case 3	1.32	-2.64	2.80	-2.37	0.6404	0.3970
Case 4	2.80	-2.37	1.32	-2.64	0.6185	0.3927

Table 2. Comparison between the authors' results and Dissanayake (1991)

As indicated in Table 2, the proposed GA method provided enhanced planning results for all the cases. Table 3 lists the numeric values for the near time-optimal motion for the two DOF arm, as presented by the *Matlab* plots. Interested readers may verify this results by using the Runge-Kutta routine in *Matlab* to calculate $\dot{\theta}_1,\dot{\theta}_2,\ddot{\theta}_1,\ddot{\theta}_2,\theta_1,\theta_2$ from the dynamic model (equation (1)) by inputting torques τ_1, τ_2.

Sahar & Hollerbach Case 1		
time (sec)	τ_1	τ_2
0.0000	342.5969	100.0000
0.0904	342.5969	100.0000
0.1726	350.0000	91.3407
0.2499	340.4026	100.0000
0.3226	317.9274	100.0000
0.3908	293.8778	100.0000
0.4543	338.8647	100.0000
0.5144	350.0000	19.6761
0.5634	350.0000	-61.0798
0.6148	350.0000	-67.0696
0.6684	350.0000	-46.8678
0.7256	350.0000	-9.6502
0.7856	350.0000	11.6812
0.8457	350.0000	33.0049
0.9003	-350.000	-41.2388
0.9552	-288.104	-36.8233
1.0218	-288.104	-36.8233

Dissanayake et all Case 1		
time (sec)	τ_1	τ_2
0.0000	10.0000	1.1693
0.0327	10.0000	2.4618
0.0633	10.0000	3.1359
0.0918	10.0000	4.7744
0.1182	10.0000	5.7809
0.1425	10.0000	7.8743
0.1649	10.0000	9.0302
0.1855	7.9105	10.0000
0.2045	-10.0000	-0.8503
0.2236	-10.0000	-3.3573
0.2444	-10.0000	-4.5338
0.2669	-10.0000	-6.1837
0.2912	-10.0000	-6.6723
0.3173	-10.0000	-7.6511
0.3451	-10.0000	-8.0005
0.3745	-10.0000	-9.1439
0.4046	-10.0000	-9.1439

Table 3. Numeric values of the optimal motion

4.2 Detailed results for Sahar and Hollerbach — case 1

The joint actuators' bound torques are set at $(\pm350;\pm100)$ and the dynamic model is presented earlier.

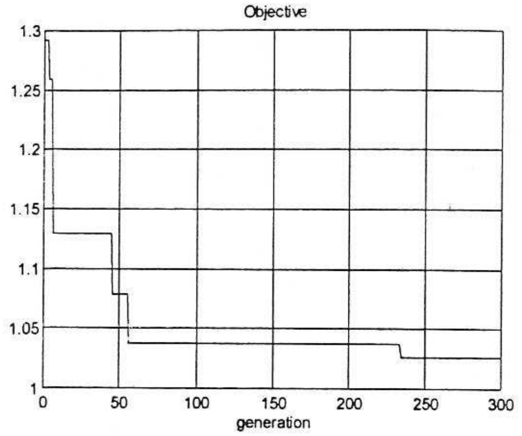

Figure 8 Objective history

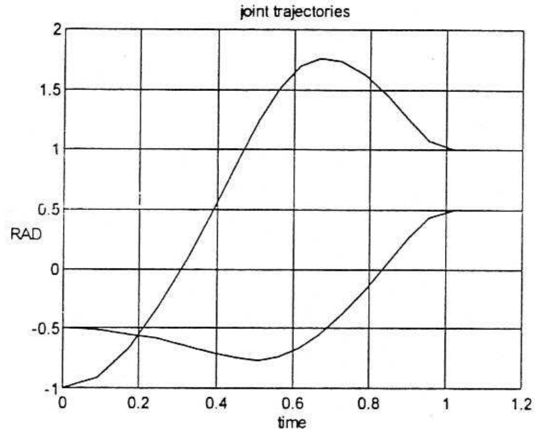

Figure 9 Near minimum-time path for Sahar and Hollerbach model

Note that Joint 1 actually moves backward to allow joint 2 forward fast motion. Joint 2 again moves inwards resulting in reduced as in the previous simulation case.

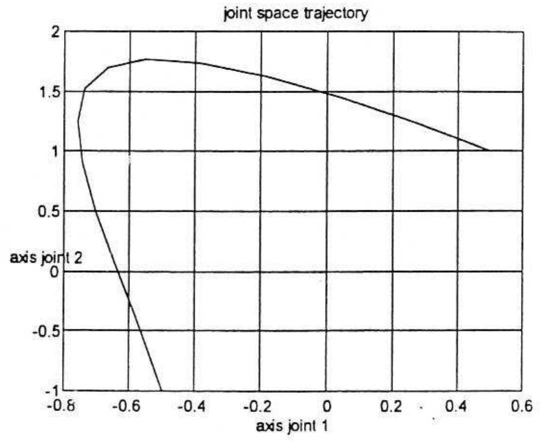

Figure 10 Time-optimal trajectory in joint space

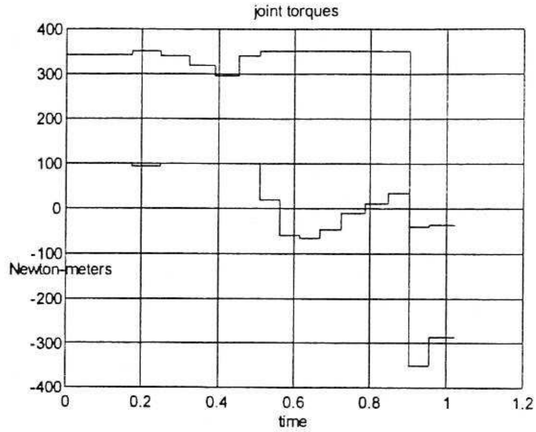

Figure 11 Joint torques

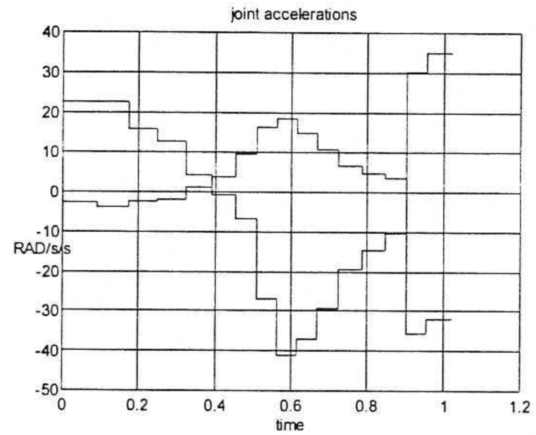

Figure 12 Joint accelerations

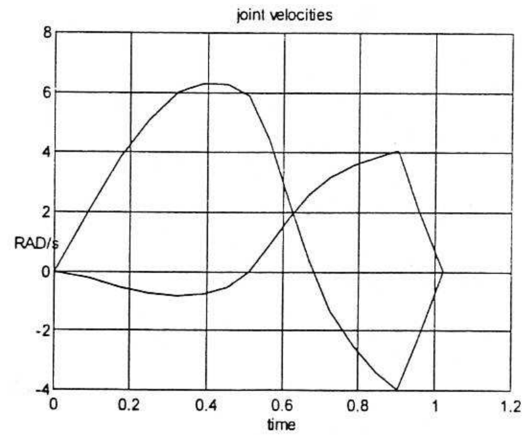

Figure 13 Joint velocities

	Initial	positions	Final	positions		
	θ_{10} (RAD)	θ_{20} (RAD)	θ_{1f} (RAD)	θ_{2f} (RAD)	Reported results	Authors' results
Case 1	-0.50	-1.00	0.50	1.00	0.8360	1.0218
Case 2	0.00	0.00	-1.05	2.10	0.5250	0.5170

Table 4. Comparison between the authors' results and Sahar & Hollerbach (1986)

Figs. (8-13) show the simulation results for two DOF robot arm but with different dynamic parameters from the last section, and Table 4 lists simulation results for two cases. It can be noted from the figures that the near minimum-time motion is searched at generation 240, which only takes about five minutes on the workstation. Fig. 10 shows that the time-optimal motion is far from a straight line. The switch position is this case was found to be 14.

4.3 Detailed result for PUMA560

In this section, simulation results are reported for the PUMA 560 arm considering different objective functions. The start and end positions used, also the boundary torque information, in all seven case studies for all six joints are given in Table 5.

	Joint 1	Joint 2	Joint 3	Joint 4	Joint 5	Joint 6
Start	-0.3	0.4	-0.18	0.0	-0.05	0.05
End	0.51	-0.42	0.58	0.87	0.64	0.84
Boundary Torque	±97.6	±186.4	±89.4	±24.2	±20.1	±97.6

Table 5 The motion start and end points (radians)

The first case study considers time optimisation with velocity constraints, and the best objective value was 0.431 seconds. Although the discrete path points have been acquired using the genetic algorithms, a spline technique (straight line linkage is the simplest linear method) has to be used to link these points together so as to provide the joint angular information in every 28 ms or other interfacing period e.g. 1.75 ms for experimentation.

Case no.	Grid size	Optimisation Criteria			Parameters		Motion
		Time	Torque	Velocity constraints	λ_τ	λ_v	Time (sec)
1	16x16	Yes	No	Yes	—	0.1	0.431
2	16x16	Yes	No	No	—	—	0.475
3	16x16	No	Yes	Yes	0.06	0.1	0.502
4	16x16	No	Yes	No	0.06	—	0.307
5	16x16	Yes	Yes	Yes	0.06	0.1	0.873
6	16x16	Yes	Yes	No	0.06	—	0.367
7	25x25	Yes	No	Yes	—	0.1	0.421

Table 6 Simulation results of different case studies for the PUMA

To provide for a study of the effect of using different combined optimisation criteria in robot motion planning, other case studies are included along with the above, as indicated in Table 6. One important parameter in any algorithm using grid search is the actual size of the grid representing the searched space, and the complexity of the search increases exponentially with the number of points in a chosen grid. Thus, it is always sensible to have a certain trade-off between search resolution and computation time. The results of case study 7 were obtained after running the simulation over around five days, as compared to the other cases for which simulations were accomplished in about one hour. In addition, case 7 was limited to 50,000 iterations to obtain the shown results, as compared to a limited iterations for the other cases. Nonetheless, the increase in minimising the motion time is relatively small (i.e. 0.421 seconds compared to 0.431 seconds) which appears to query the benefit of the increase in the grid size. As expected, all cases where the optimisation is constrained by a near-zero end-point velocity exhibit a higher motion time. The consideration of such a constrain may however be important if motion is to be planned via successive segments, as it is the case for a point-look-ahead motion planner.

The motion profiles for all six joints of the PUMA are shown in Fig. 14-18 for case 1 of Table 6. In the figures, the solid line is for joint 1, the dashed line for joint 2, the dash-dotted line for joint 3, the star * line for joint 4, the plus + line for joint 5 and the plus x line for joint 6.

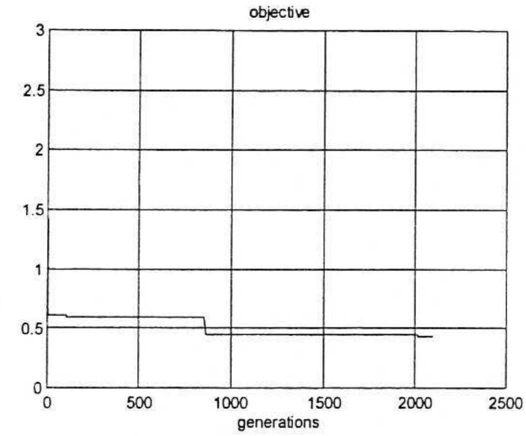

Figure 14 Generation history

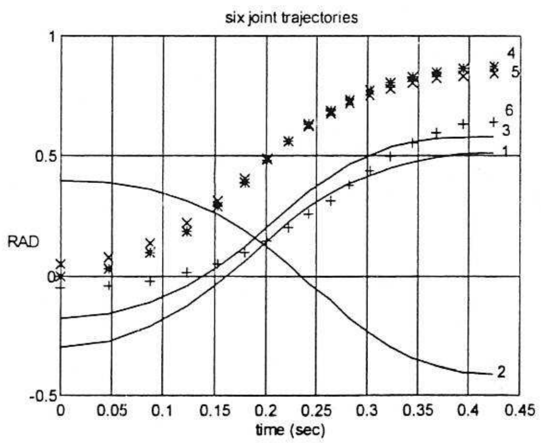

Figure 15 Near minimum-time PUMA motion

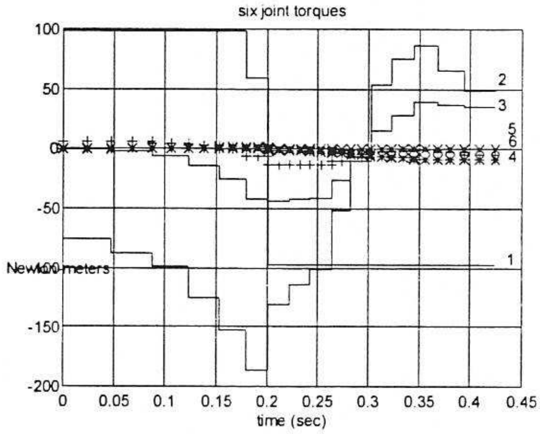

Figure 16 Six torques

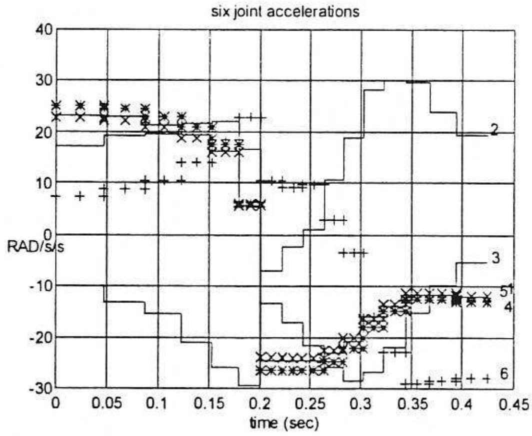

Figure 17 Six accelerations

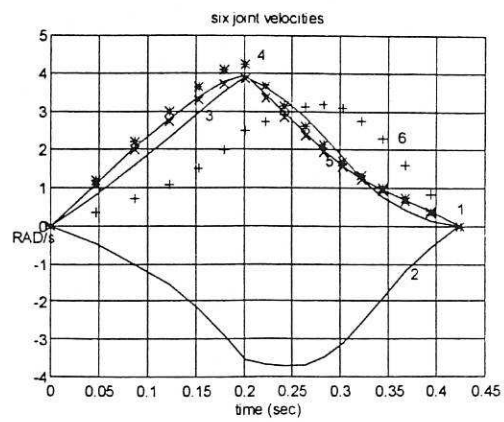

Figure 18 Six velocities

5. CONCLUSIONS

This work reported on comparisons between a genetic based motion planner and other heuristic and dynamic control methods. Results are reported for 2-joint and 6-joint articulated arms. In addition, a heuristic search based on the dynamic scaling scheme is introduced, based on the assumption that the torque only switches once during the whole motion. Much better results are acquired than those reported in Dissanayake (1991) and Sahar and Hollerbach (1986). Simulations show the trade-off between the search time and the search accuracy, and gives some insight into the choice of the grid size. While a large grid size may yield more optimal search results, the search time does increase considerably (an hour to a few days)..

ACKNOWLEDGEMENT

This work is supported by EPSRC (grant GRJ/15797).

REFERENCES

1. Chan K K and Zalzala A M S (1993), "Genetic-Based Motion Planning of Articulated Robotic Manipulators with Torque Constraints", IEE Colloquium on Genetic Algorithms for Control and System Engr., London, May.
2. Zalzala A M S and Chan K K (1994), "An Evolutionary Solution for the Control of Mechanical Arms", ICARCV'94 3rd Int. Conf. Automation, Robotics & Comp. Vision, 8-11 Nov., Singapore.
3. Chen, M. and Zalzala, A.M.S., "Dynamic modelling and genetic-based motion planning of mobile manipulator systems with nonholonomic constraints", Control Engineering Practice, Vol. 5, No. 1, pp. 39-48, 1997.
4. Sun, S., Morris, A.S. and Zalzala, A.M.S., "Trajectory planning of multiple co-ordinating robots using genetic algorithms", *Robotica*, Vol.14, pp. 227-34, 1996.
5. Rana, A.S. and Zalzala, A.M.S., "Near time-optimal collision-free motion planning of robotic manipulators using an evolutionary algorithm", Robotica, Vol. 14, pp. 621-32, 1996.
6. Wang, Q. and Zalzala, A.M.S., "Genetic algorithms for PUMA robot motion control: A practical implementation" , *Int. J. Mechatronics*, Vol.6, No.3, pp 349-65, 1996.
7. Wang, Q. and Zalzala, "Investigations into robotic multi-joint motion considering multi-criteria optimisation using genetic algorithms", In *Proc. IFAC World Congress,* Vol.A, pp. 301-6, San Fransisco, 1996.
8. Wang, Q. and Zalzala, A.M.S., "Genetic control of near time optimal motion for an industrial robot arm", In *Proc. IEEE Int Conf on Robotics and Automation*, Vol.3, pp. 2592-7, 1996.
9. Wang, Q. and Zalzala, A.M.S., "Investigations into the decoding of genetic based robot motion considering sequential and parallel formulations", In *Proc. UKACC Int Conf on Control*, Vol.1, pp. 442-7, Exeter, 1996.
10. Dissanayake M W M G, Goh G J and Phan-Thien N (1991), "Time-optimal trajectories for robot manipulators", Robotica, vol.9, pp131-138.
11. Hollerbach J M (1984), "Dynamic Scaling of Manipulator Trajectories", J. of Dynamic Systems, Measurement, & Control, T. of ASME, vol106, March, pp102-106.
12. Sahar G, Hollerbach J M (1986), "Planning of Minimum-Time Trajectory for Robot Arms", Int. J. Robotics Res., MIT Press, Vol.5 No. 3 pp.91-100.
13. Shiller Z and Dubowsky (1989), "Robot Path Planning with Obstacles, Actuator, Gripper and Payload Constraints", Int. J. Robotics Res., vol.8, No. 6, Dec. 1989, pp3-18.